



**JINR**

**LXX International conference "NUCLEUS – 2020.  
Nuclear physics and elementary particle physics.  
Nuclear physics technologies"**



# **Simulation of 14 MeV neutron scattering on titanium, chromium and iron nuclei**

**I.D. Dashkov on behalf of TANGRA collaboration**

**15.10.2020**

# Motivation and objects of research

Z	52Fe 8.275 H ε: 100.00%	53Fe 8.51 M ε: 100.00%	54Fe STABLE 5.845%	55Fe 2.744 Y ε: 100.00%	56Fe STABLE 91.754%
25	51Mn 46.2 M ε: 100.00%	52Mn 5.591 D ε: 100.00%	53Mn 3.74E+6 Y ε: 100.00%	54Mn 312.20 D ε: 100.00% β-: 9.3E-5%	55Mn STABLE 100%
24	50Cr >1.3E+18 Y 4.345% 2ε	51Cr 27.7025 D ε: 100.00%	52Cr STABLE 83.789%	53Cr STABLE 9.501%	54Cr STABLE 2.365%
23	49V 330 D ε: 100.00%	50V >2.1E+17 Y 0.250% ε > 92.90% β- < 7.10%	51V STABLE 99.750%	52V 3.743 M β-: 100.00%	53V 1.543 M β-: 100.00%
22	48Ti STABLE 73.72%	49Ti STABLE 5.41%	50Ti STABLE 5.18%	51Ti 5.76 M β-: 100.00%	52Ti 1.7 M β-: 100.00%
	26	27	28	29	N

- $^{nat}\text{Ti}$ ,  $^{nat}\text{Cr}$ ,  $^{nat}\text{Fe}$  are structural materials for the IV generation fast neutron reactors. Data on scattering of fast neutrons is important for calculating future reactor characteristics.
- TANGRA collaboration studies fast neutron ( $E_n = 14.1$  MeV) scattering on samples of different elements
- For model description of TANGRA experimental data, it is necessary to check sensitivity of TALYS 1.9 calculations to model variation and it's correspondence to database evaluations.

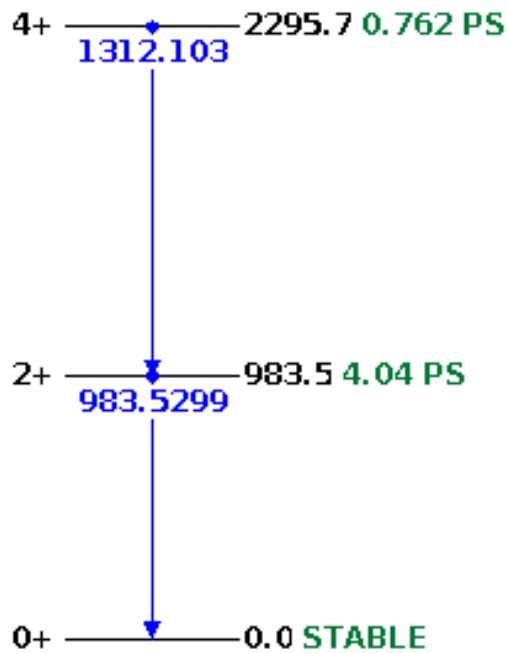
$^{46}\text{Ti}$  (8.0%),  $^{47}\text{Ti}$  (7.8%),  $^{48}\text{Ti}$  (**73.5%**),  $^{49}\text{Ti}$  (5.1%),  $^{50}\text{Ti}$  (5.3%)

$^{50}\text{Cr}$  (4.4%),  $^{52}\text{Cr}$  (**83.8%**),  $^{53}\text{Cr}$  (9.5%),  $^{54}\text{Cr}$  (2.4%)

$^{54}\text{Fe}$  (5.9%),  $^{56}\text{Fe}$  (**91.8%**),  $^{57}\text{Fe}$  (2.1%),  $^{58}\text{Fe}$  (0.3%)

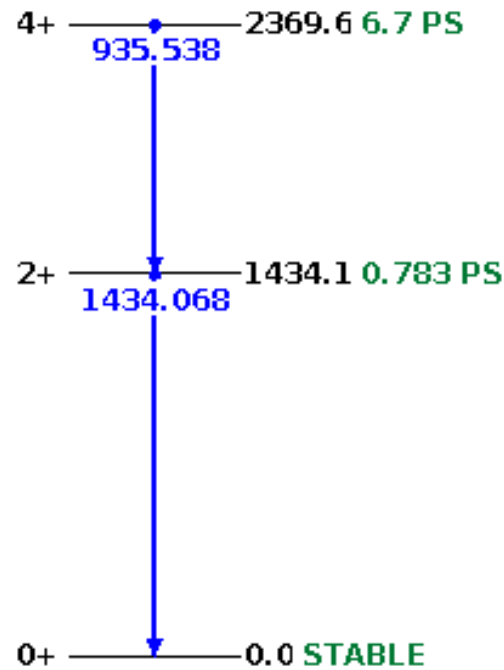
The most abundant isotopes give the greatest contribution to the reaction cross sections. Influence from other isotopes can be considered negligible.

# Low-lying levels of $^{48}\text{Ti}$ , $^{52}\text{Cr}$ , $^{56}\text{Fe}$



$^{48}_{22}\text{Ti}_{26}$  [1]

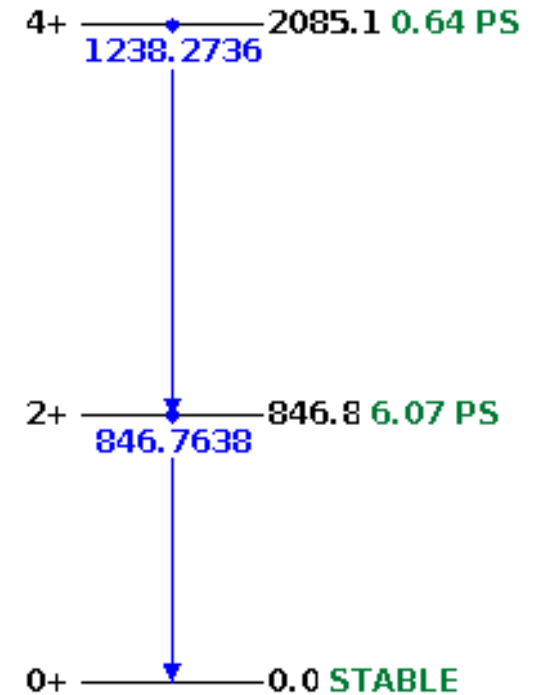
$$E_{4+}/E_{2+} = 2.33$$



$^{52}_{24}\text{Cr}_{28}$  [2]

$$E_{4+}/E_{2+} = 1.65$$

There is magical number of neutrons in  $^{52}\text{Cr}$ :  $N = 28$



$^{56}_{26}\text{Fe}_{30}$  [3]

$$E_{4+}/E_{2+} = 2.46$$

In coupled-channels calculations with vibrational approach, it was decided to use  $(0_{g.s.}^+, 2_1^+)$  coupling, where the  $2_1^+$  level is a one-quadrupole phonon excitation.

1. T. W. Burrows, Nucl. Data Sheets 107, 1747 (2006).

2. Yang Dong, Huo Junde Nucl. Data Sheets 128, 185 (2015).

3. Huo Junde, Huo Su, Yang Dong Citation: Nucl. Data Sheets 112, 1513 (2011).

# Calculation approaches and nuclei deformation parameters

For  $^{48}\text{Ti}$ ,  $^{52}\text{Cr}$ ,  $^{56}\text{Fe}$  calculations with three approaches for nucleus collectivity were performed: DWBA, CC with rotational and vibrational types of nuclear levels excitation for default TALYS 1.9 deformation parameters.

TALYS 1.9 deformation parameters for  $^{48}\text{Ti}$ ,  $^{52}\text{Cr}$ ,  $^{56}\text{Fe}$  for their first excited states are given in the table and compared with  $\beta_2$  parameters from CDFE database.

Note, that default approach for  $^{52}\text{Cr}$  include several levels that are treated as vibrational, thus rotational-vibrational approach is invoked.

	TALYS 1.9		CDFE database	
	$\beta_2$ ( $\beta_4$ ) for $2^+_{1}$ state	Default approach	$\beta_2(B(E2)\uparrow)$	$\beta_2(Q_{\text{mom}})$
$^{48}\text{Ti}$	+0.269 (0.0)	DWBA	$0.269 \pm 0.007$ [4]	$+0.168 \pm 0.016$ [5]
$^{52}\text{Cr}$	+0.223 (+0.077)	Rotational-vibrational	$0.224 \pm 0.005$ [4]	$+0.067 \pm 0.02$ [6]
$^{56}\text{Fe}$	+0.239 (0.0)	DWBA	$0.2393 \pm 0.0049$ [4]	$+0.171 \pm 0.031$ [7] $+0.141 \pm 0.066$ [8]

4. Raman *et al.* At. Data Nucl. Data Tables 78 (2001), 1

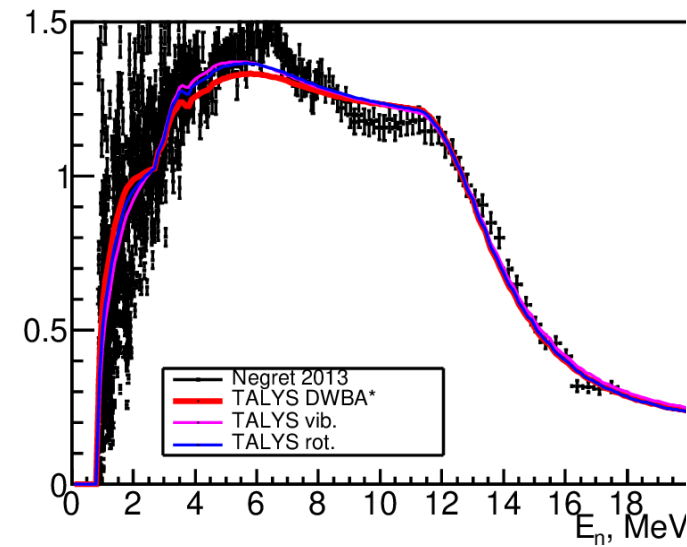
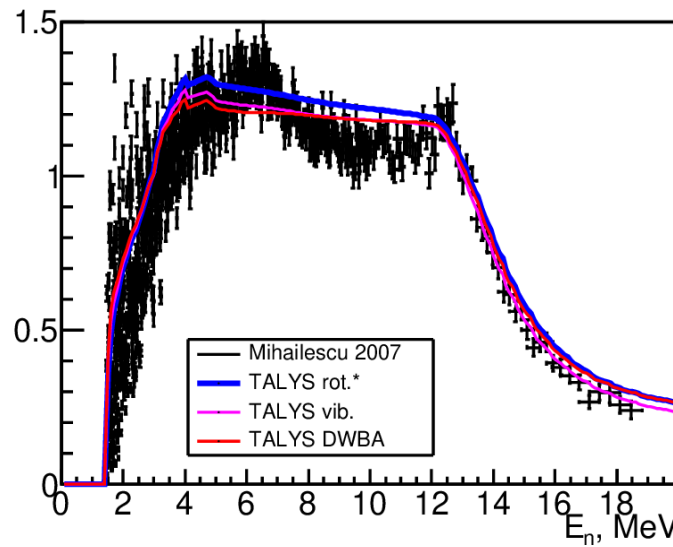
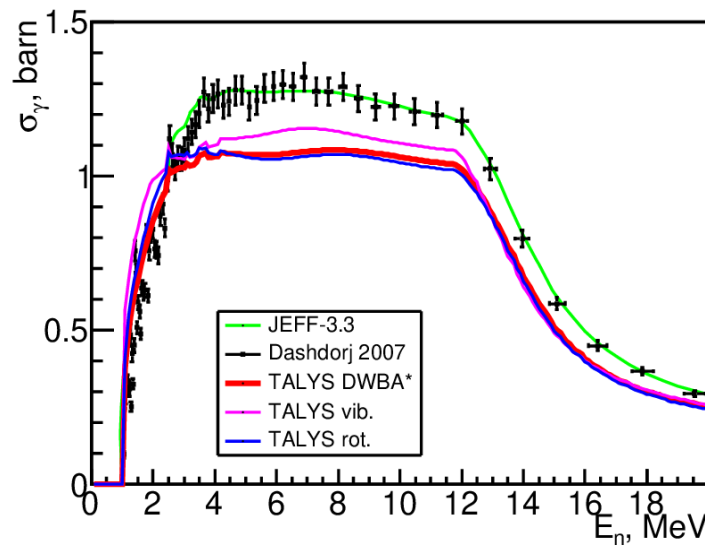
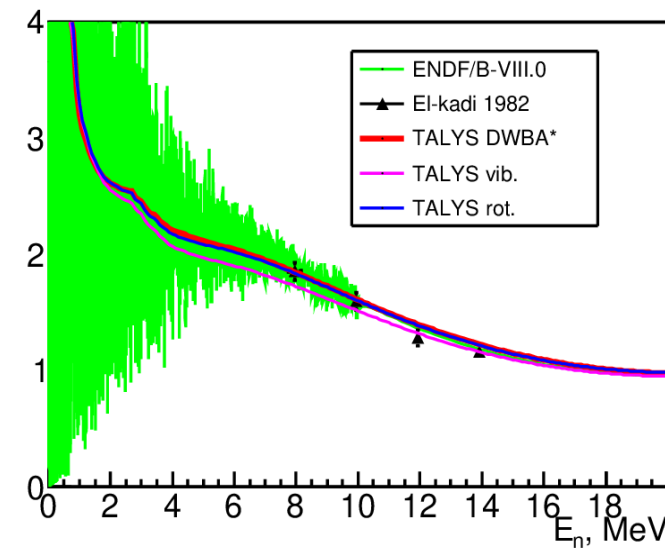
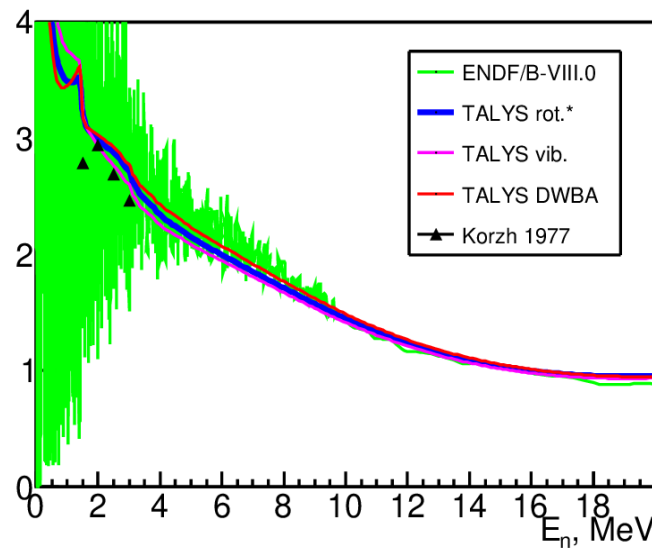
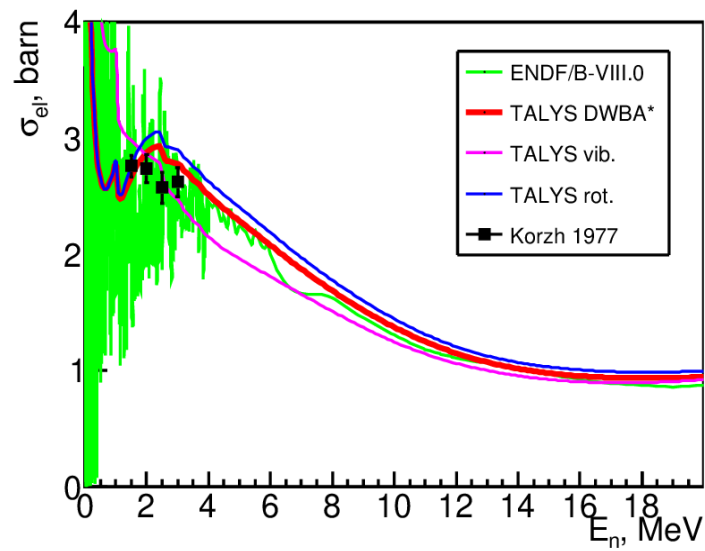
5. Lightbody. Phys. Lett. 38B (1972), 475

6. Raghavan At. Data Nucl. Data Tables 42 (1989), 189

7. Thomson *et al.* Phys. Rev. C4 (1971) , 1699

8. LeVine *et al.* Phys. Rev. C23 (1981), 244

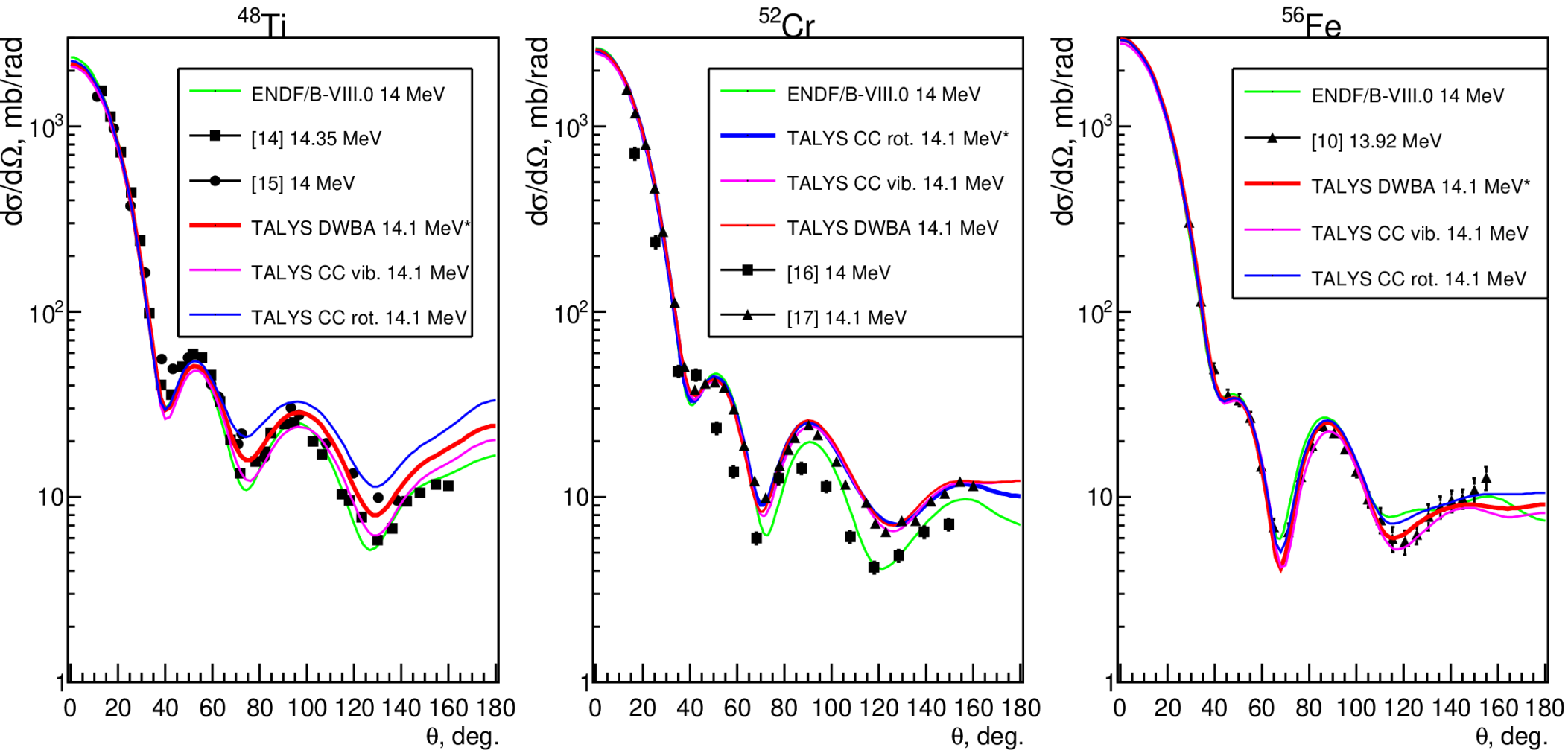
# Elastic $\sigma_{el}$ and $2^+_1 \rightarrow 0^+_{g.s}$ $\gamma$ -transition $\sigma_\gamma$ cross sections versus $E_n$



9. Korzh, et al. Ukr. Fiz. Zh 22 (1977), 112
10. El-Kadi, et al. Nuclear Physics A 390.3(1982), 509
11. Negret, et al. Phys. Rev. C 88, (2013) 027601
12. Dashdorj, et al. Nuclear Science and Engineering 157, 65 (2007)
13. Mihailescu, et al. NPA 786, (2007) 1

(asterisk in a legend marks default TALYS 1.9 parameters)

# Angular distribution of elastically scattered neutrons



Differential cross sections of elastically scattered neutrons for  $^{48}\text{Ti}$ ,  $^{52}\text{Cr}$ ,  $^{56}\text{Fe}$  are plotted versus scattering angle in center of mass system. The spread of experimental data points makes it difficult to conclude what model approach is the best for  $^{48}\text{Ti}$ . Vibrational approach seems to be the closest one to the more recent experimental data [26] for  $^{48}\text{Ti}$ , while rotational approach is unable to correctly reproduce cross section for angles greater than  $60^\circ$

14. Schmidt D., et al. CM-P00061940, report PTB-N-50 (2006).

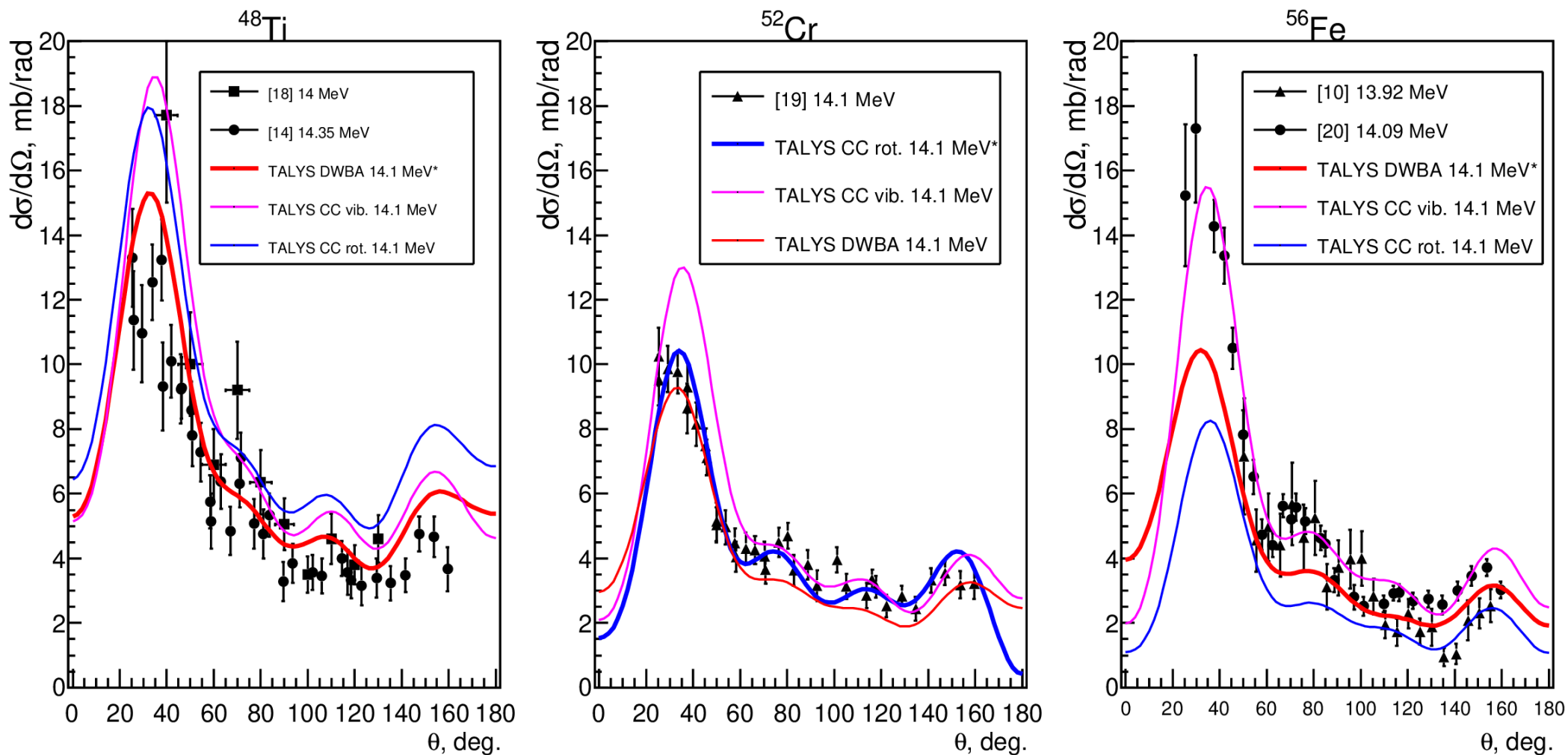
15. Pierre C. S., et al. Phys. Rev. 115, Issue. 4., p.999 (1959).

16. Christodoulou E. G., et al. Nuclear science and engineering 132, №. 3., p.273 (1999).

17. Han Yin-Lu, Chinese Physics C 28, №. 5., p.512 (2004).

(Asterisk in a legend marks default TALYS 1.9 parameters)

# Angular distribution of inelastically scattered neutrons (to the $2^+_1$ state)



Differential cross sections of inelastically scattered neutrons for  $^{48}\text{Ti}$ ,  $^{52}\text{Cr}$ ,  $^{56}\text{Fe}$  are plotted versus scattering angle in center of mass system. Vibrational approach seems to be the closest one to the recent experimental data [30] for  $^{48}\text{Ti}$ . For  $^{56}\text{Fe}$  vibrational approach is capable of recreating the cross section for small angles below  $50^\circ$ .

18. Leshchenko B.E., et al. Yadernaya Fizika, Vol.15, Issue.1, p.10 (1972).

19. Schmidt D., et al. Phys.Techn.Bundesanst., Neutronenphysik Reports, No.31 (1998).

20. Schmidt D., et al. Phys.Techn.Bundesanst., Neutronenphysik Reports, No.20 (1994).

(Asterisk in a legend marks default TALYS 1.9 parameters)

# Integral cross sections calculations results comparison

To conclude the most appropriate approach from the considered for the 0-20 MeV energy range, standard deviations  $D$  from experimental or evaluated data points were calculated. Deviations for  $\sigma_{\text{tot}}$ ,  $\sigma_{\text{el}}$ ,  $\sigma_{\text{inel}}$ ,  $\sigma_{\text{y}}$ ,  $(\sigma/\Omega)_{\text{el}}$ , and  $(\sigma/\Omega)_{\text{inel}}$  are presented the tables.

		DWBA	CC rotational	CC vibrational
$\sigma_{\text{tot}}$	$^{48}\text{Ti}$	<b>192</b>	233	230
	$^{52}\text{Cr}$	309	<b>300</b>	331
	$^{56}\text{Fe}$	533	529	<b>503</b>
$\sigma_{\text{el}}$	$^{48}\text{Ti}$	<b>184</b>	232	224
	$^{52}\text{Cr}$	<b>298</b>	303	330
	$^{56}\text{Fe}$	<b>494</b>	500	497
$\sigma_{\text{inel}}$	$^{48}\text{Ti}$	<b>71</b>	88	82
	$^{52}\text{Cr}$	<b>78</b>	86	81
	$^{56}\text{Fe}$	132	143	<b>130</b>
$\sigma_{\text{y}}$	$^{48}\text{Ti}$	139	151	<b>122</b>
	$^{52}\text{Cr}$	<b>90</b>	109	<b>90</b>
	$^{56}\text{Fe}$	<b>152</b>	160	155

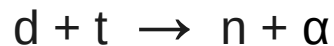
		DWBA	CC rotational	CC vibrational
$(\sigma/\Omega)_{\text{el}}$	$^{48}\text{Ti}$	27	<b>18</b>	39
	$^{52}\text{Cr}$	<b>11.0</b>	11.1	23.7
	$^{56}\text{Fe}$	34.3	21.6	<b>18</b>
$(\sigma/\Omega)_{\text{inel}}$	$^{48}\text{Ti}$	<b>1.7</b>	3.3	3.6
	$^{52}\text{Cr}$	1.6	<b>0.7</b>	1.8
	$^{56}\text{Fe}$	2.4	<b>0.9</b>	1.0

	Our choice	Default
$^{48}\text{Ti}$	DWBA	DWBA
$^{52}\text{Cr}$	DWBA	CC rot.
$^{56}\text{Fe}$	CC vib.	DWBA



# Fast neutron scattering on TANGRA setup

- TANGRA setup register  $\gamma$ -quanta emitted from  $(n, X\gamma)$  reactions induced by fast 14.1 MeV neutrons.
- Compact neutron generator ING-27 has inbuilt  $\alpha$ -particles detector.
- The tagged neutron method (TNM) is based on registration in coincidences with the  $\alpha$ -particles, formed in a binary reaction, which produces the neutrons:



- Using of the TNM improves the signal/background ratio.
- The setup allows one to measure the yields or cross-sections of gamma transitions. This data can be used for nuclear model validation.

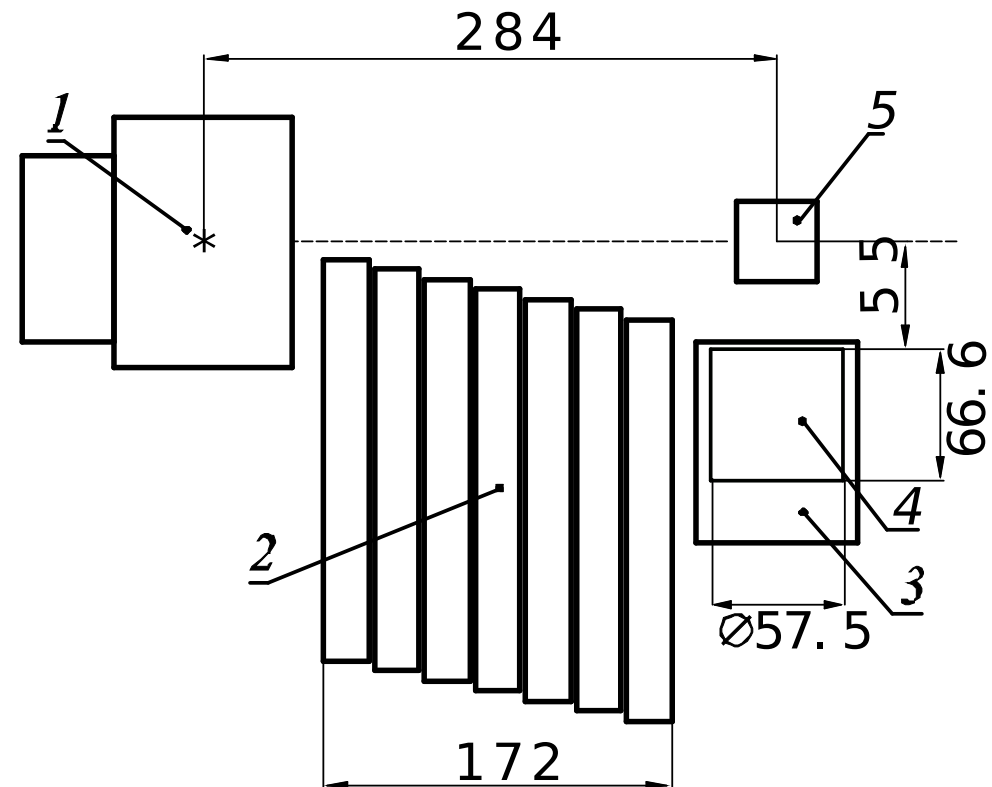


Fig. 2. Scheme of the TANGRA setup with the HPGe detector in the reaction plane: 1 - neutron generator ING-27, 2 - lead shielding, 3 - case of the HPGe detector, 4 - HPGe crystal, 5 - sample. Axis of the experimental setup is indicated by horizontal dashed line. Tritium-enriched target is marked as asterisk. All dimensions are in mm.

# $\gamma$ -emission spectra obtained on TANGRA setup

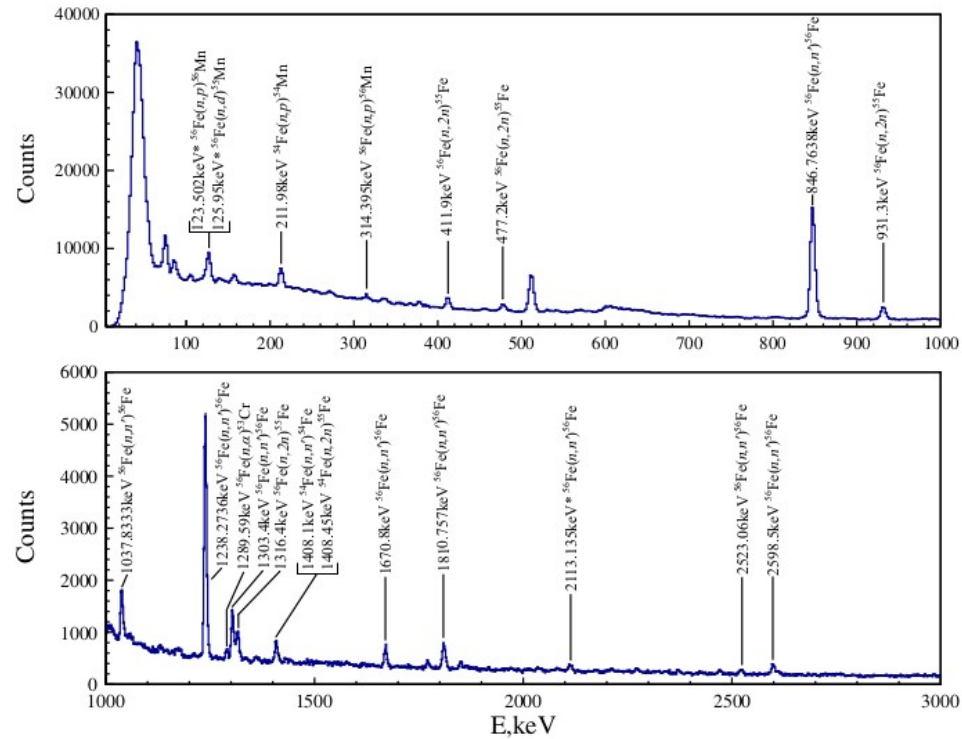


Fig. 3. Gamma-spectrum obtained by irradiating a Fe sample with 14.1 MeV neutrons.

See talk tomorrow Fedorov, et al. «Measurements of the  $\gamma$  ray emission cross-sections in Fe(n,xy)-type reactions», 16.10.20, 16:00, Sec. 2

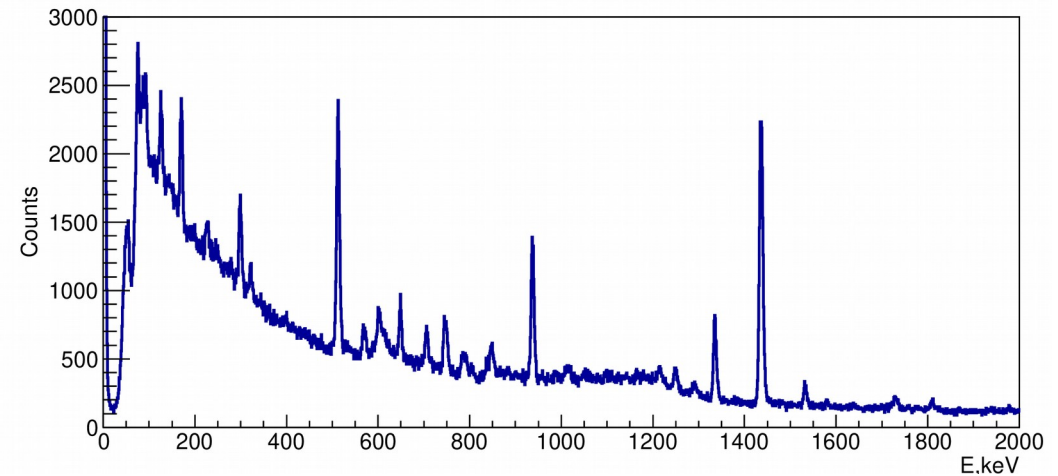


Fig. 4. Gamma-spectrum obtained by irradiating a Cr sample with 14.1 MeV neutrons.

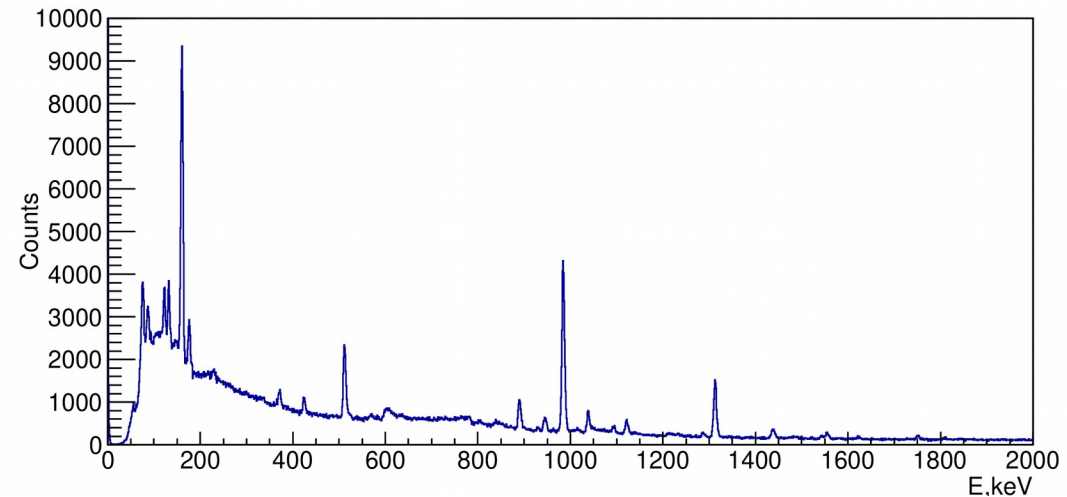


Fig. 5. Gamma-spectrum obtained by irradiating a Ti sample with 14.1 MeV neutrons.

# $\gamma$ -transition yields in (n,n') reaction on $^{48}\text{Ti}$

$E_\gamma$ , keV	$J_i^P \rightarrow J_f^P$	TANGRA			[21]			[12]			TALYS 1.9
		14.1 MeV			14.5 MeV			13.96 MeV			14.1 MeV
			$\pm$			$\pm$			$\pm$		DWBA*
423.6	$4_1^- \rightarrow 3_1^-$	4.9	$\pm$	0.4				4.1	$\pm$	0.2	1.8
944.1	$4_2^+ \rightarrow 4_1^+$	7.5	$\pm$	0.2	7.1	$\pm$	0.9	7.6	$\pm$	0.3	4.6
983.5	$2_1^+ \rightarrow 0_{\text{g.s.}}^+$	100.0	$\pm$	0.5	100.0	$\pm$	9.2	100.0	$\pm$	3.4	100.0
1037.5	$6_1^+ \rightarrow 4_1^+$	10.8	$\pm$	0.3				0.9	$\pm$	0.1	9.6
1312.1	$4_1^+ \rightarrow 2_1^+$	40.0	$\pm$	0.4	35.7	$\pm$	4.1	42.6	$\pm$	1.5	41.0
1437.5	$2_2^+ \rightarrow 2_1^+$	7.5	$\pm$	0.2	7.4	$\pm$	1.1	6.0	$\pm$	0.2	4.8
1750.3	$5_1^- \rightarrow 4_1^+$	3.2	$\pm$	0.2	3.5	$\pm$	2.0	4.0	$\pm$	0.2	2.3
2240.4	$3_1^+ \rightarrow 2_1^+$	2.9	$\pm$	0.4	4.8	$\pm$	0.8	2.8	$\pm$	0.2	2.7
2387.3	$2_4^+ \rightarrow 2_1^+$	2.0	$\pm$	0.2				2.2	$\pm$	0.1	1.1

(Asterisk in a table marks default TALYS 1.9 parameters)

# $\gamma$ -transition yields in (n,n') reaction on $^{52}\text{Cr}$

Ey, keV	$J_i^P \rightarrow J_f^P$	TANGRA [22]		[13]		[23]			[24]			TALYS 1.9
		14.1 MeV		~14 MeV		14.2 MeV			14.8 MeV			DWBA
647.5	$4_3^+ \rightarrow 4_2^+$	9.9	$\pm 0.4$	9.0	$\pm 1.9$							4.2
744.2	$6_1^+ \rightarrow 4_1^+$	11.7	$\pm 0.4$	6.3	$\pm 1.3$				17.4	$\pm 3.1$		8.1
935.5	$4_1^+ \rightarrow 2_1^+$	32.3	$\pm 0.5$	33.5	$\pm 3.2$	29.2	$\pm 4.6$		28.6	$\pm 4.1$		32.4
1212.8	$0_2^+ \rightarrow 2_1^+$	4.9	$\pm 0.4$	1.7	$\pm 0.9$				21.5	$\pm 4.2$		2.6
1246.3	$5_1^+ \rightarrow 4_1^+$	5.9	$\pm 0.4$	1.7	$\pm 0.3$							2.8
1333.6	$5_1^- \rightarrow 4_1^+$	25.5	$\pm 0.5$	25.1	$\pm 2.9$	31.6	$\pm 5.3$		23.5	$\pm 4.2$		20.8
1434.1	$2_1^+ \rightarrow 0_{g.s.}^+$	100.0	$\pm 1.1$	100.0	$\pm 7.5$	100.0	$\pm 10.5$		100.0	$\pm 9.9$		100.0
1530.7	$2_2^+ \rightarrow 2_1^+$	6.9	$\pm 0.3$	6.6	$\pm 0.9$				10.1	$\pm 3.1$		4.1
1727.5	$2_3^+ \rightarrow 2_1^+$	5.0	$\pm 0.3$	4.5	$\pm 0.9$							2.5
2038.2	$3_1^+ \rightarrow 2_1^+$	2.3	$\pm 0.4$	1.5	$\pm 0.7$							1.5
2337.4	$2_4^+ \rightarrow 2_1^+$	1.8	$\pm 0.4$	2.1	$\pm 0.9$							2.4

22. Grozdanov, et. al. Yadernaya Fizika 83, (2020) 200

23. Abbondanno, et al., J. Nucl. Energy. 27, (1973) 227

24. Yamamoto, et al. J. Nucl. Science and Technology. V.15:11, (1978) 797

(Asterisk in a table marks default TALYS 1.9 parameters)

# $\gamma$ -transition yields in (n,n') reaction on $^{56}\text{Fe}$

$E_{\gamma}$ , keV	$J_i^P \rightarrow J_f^P$	TANGRA		[11]		TALYS 1.9
		14.1 MeV		14.5 MeV		14.1 MeV CC vib.
846.8	$2_1^+ \rightarrow 0_{\text{g.s.}}^+$	100.0	$\pm 0$	100.0	$\pm 0$	100
1037.8	$4_2^+ \rightarrow 4_1^+$	8.2	$\pm 0.8$	6.0	$\pm 0.5$	6.6
1238.3	$4_1^+ \rightarrow 2_1^+$	43.8	$\pm 1.1$	36.0	$\pm 0.2$	48.7
1303.4	$6_1^+ \rightarrow 4_1^+$	9.2	$\pm 0.6$	9.3	$\pm 0.6$	9.5
1670.8	$6_2^+ \rightarrow 4_1^+$	4.5	$\pm 0.5$	6.9	$\pm 0.7$	5
1810.8	$2_2^+ \rightarrow 2_1^+$	6.7	$\pm 0.5$	4.8	$\pm 0.6$	3
2113.1	$2_3^+ \rightarrow 2_1^+$	2.5	$\pm 0.7$	1.9	$\pm 0.6$	1.9
2523.1	$2_4^+ \rightarrow 2_1^+$	2.5	$\pm 0.8$	2.7	$\pm 0.6$	1
2598.5	$3_1^+ \rightarrow 2_1^+$	3.4	$\pm 0.5$	4.5	$\pm 0.6$	2.1

# Conclusions

- New experimental results for  $\gamma$ -yields on  $^{48}\text{Ti}$ ,  $^{52}\text{Cr}$   $^{56}\text{Fe}$  were obtained on the TANGRA facility with the TNM for 14.1 MeV neutron induced reactions. The results were in good agreement with other experimental data, except ones for several  $\gamma$ -lines.
- Nuclear reaction code TALYS 1.9 was used for checking up the calculation sensitivity to changes in model approach. Calculations for DWBA model, CC model in rotational and vibrational approaches were performed for same deformation and optical model parameters.
- DWBA model was considered the most appropriate for  $^{48}\text{Ti}$  and  $^{52}\text{Cr}$ , CC with vibrational level excitation was chosen for  $^{56}\text{Fe}$ .
- TALYS 1.9 calculated  $\gamma$ -yields were in good agreement with our experimental data. Calculation results for considered approaches showed no significant difference for  $\gamma$ -yields, but varied for integral and differential cross sections.